

# An Experimental Study on Various Combinations of Shape Descriptors and Matching Methods Applied in the General Shape Analysis Problem

Katarzyna Gościewska\*  
Supervised by: Dariusz Frejlichowski†

West Pomeranian University of Technology, Szczecin,  
Faculty of Computer Science and Information Technology,  
Żołnierska 52, 71-210, Szczecin, Poland

## Abstract

The aim of the General Shape Analysis (GSA) is to find one or a few most similar general templates for a processed object — exact identification is not performed, but the general shape features are obtained. The GSA approach may be applied for coarse separation of objects in the database prior to their classification or in the case when the data are incomplete or there is a high variability within them. In this paper, the GSA problem is investigated using various combinations of shape descriptors and methods for estimating the similarity or dissimilarity between shape representations. The experiments involved the use of five shape descriptors, namely the Two-Dimensional Fourier Descriptor, Generic Fourier Descriptor, UNL-Fourier descriptor, Zernike Moments and Point Distance Histogram, as well as four matching methods, that is the Euclidean distance, Mahalanobis distance, correlation coefficient and C1 metric. The effectiveness of the experiments was calculated as a coincidence between experimental results and results provided by people through inquiry forms. The experiments made it possible to determine the influence of various matching methods on the final effectiveness when a particular shape descriptor was applied. The best result was obtained for the combination of UNL-Fourier descriptor and C1 metric.

**Keywords:** General Shape Analysis, shape descriptors, similarity and dissimilarity measures

## 1 Introduction

The problem of General Shape Analysis (GSA) is considered similar to typical shape recognition or shape retrieval, however both of these approaches differ in their purpose. The GSA is aimed at finding one or a few most similar general templates for each investigated test object. Usually, a template is a simple geometrical figure, e.g. a tri-

angle, rectangle or circle, whereas a test object is a more diversified shape for which the similarity to one or several templates is defined. This approach enables to determine the most general and predominant shape features. The idea of the GSA is to represent all shapes using a particular shape descriptor and calculate a similarity or dissimilarity measure between test objects and templates. Next, a set of most similar templates indicated by the algorithm is compared with the results provided by people through inquiry forms, in which they were asked to indicate five templates for each investigated object — from the most to the least similar one. The percentage convergence between the two gives the final effectiveness value of the experiment.

The General Shape Analysis was introduced in [1] and firstly applied for the Two-Dimensional Fourier Descriptor. In subsequent years, this approach has been examined with the use of other shape descriptors, among which were the UNL-Fourier descriptor [2], Generic Fourier Descriptor [3], Point Distance Histogram [2, 3], Zernike Moments [4], Moment Invariants [4] or Curvature Scale Space [5]. Based on what is known from available literature, the Euclidean distance has been used to establish shape dissimilarity. The first application of a different shape matching method was presented in [6], where the correlation coefficient was applied to match Fourier-based shape representations.

In this paper, various combinations of shape descriptors and matching methods are investigated. The shape descriptors include some of the methods mentioned above — the Two-Dimensional Fourier Descriptor, Generic Fourier Descriptor, UNL-Fourier descriptor, Zernike Moments and Point Distance Histogram, however in the paper several versions of each shape descriptor are used, i.e. feature vectors of various size. For shape matching, two dissimilarity measures were selected, namely the Euclidean distance and Mahalanobis distance, and two similarity measures — the correlation coefficient and C1 metric. This made it possible to determine the most appropriate method for solving the GSA task. Moreover, in this paper, a different approach for estimating experimental effectiveness

---

\*kgosciewska@wi.zut.edu.pl

†dfrejlichowski@wi.zut.edu.pl

is applied. Usually, the three most similar templates indicated by the algorithm and people in the inquiry forms were compared with respect to the sequence of indications. According to the suggestions included in [4], the sequence of indications is not taken into account and only the first template indicated by the algorithm is considered. Under this condition a template is proper only if it matches one out of three indications from the human benchmark result.

Some may disagree with the abovementioned manner of estimating effectiveness, arguing that human shape perception is supported by the theory of Recognition-By-Components proposed by Biederman. This theory assumes that an object is an arrangement of a number of basic components, including block, sphere, arc, cylinder or wedge, and that these components can be used to describe a shape [10]. Furthermore, it cannot be overlooked that there are other approaches to cognitive pattern recognition, such as the Theory of Template or the Theory of Feature. According to the former, people store templates in the long-term memory and use them to recognize a pattern. Contrarily, the latter one states that instead of matching the entire pattern with a template, people try to match their features [15]. It also needs to be emphasized that the General Shape Analysis is not concerned with studying the way in which people process the shape and establish the similarity between some shapes, but it investigates the results provided by people and based on them it tries to find an appropriate substitute in the area of computer pattern recognition. In addition, we should also think of how people describe things in daily life. Relatively often we define a shape of an unknown object using commonly known features — for example, we say that something is round or square or has several features in the sense that we can distinguish several known characteristics in the entire shape. Moreover, in some aspects of life, establishing an objects similarity to simple geometric figures is common and considered useful, for instance, in case of human body shape or a shape of a face, where the awareness of the shape simplifies choosing an outfit or hairstyle. Despite the triviality of this example, it is undoubtedly true that people tend to compare shapes to their simpler equivalents.

Taking into account what has been stated in the above paragraph, as well as focusing on the algorithms, the GSA approach may be applied for coarse separation of objects in the database prior to their exact classification or in the case when the data are incomplete or there is a high variability among the data. The GSA has been successfully applied in the identification of stamp types, which is useful in searching for presumably falsified digital documents [14]. The approach may also be applied in searching large multimedia databases, where voice commands are used for shape retrieval [2]. In this paper, focus is not placed on a specific application, but rather on the evaluation of the methods and algorithms.

The rest of the paper is organised as follows. The second section describes methods for estimating similarity and dissimilarity between shape representations, i.e.

methods for matching feature vectors. The third section briefly presents algorithms selected for shape representation. The fourth section provides the conditions of the experiments and experimental results concerning the application of various combinations of shape descriptor and matching method as part of the GSA task. The last section summarizes and concludes the paper.

## 2 Methods for estimating similarity and dissimilarity between shape representations

In the GSA, test objects are compared with the templates in order to estimate the similarity (or dissimilarity) between shapes. Shape similarity enables to establish the level of similarity (or dissimilarity) between two shapes. Shape similarity criteria have to be adapted to the specific problem, i.e. the shapes have to be represented using features relevant to the problem under consideration [8]. The similarity of shapes is determined through matching a shape and calculated measure. In this paper, four measures are investigated — two similarity and two dissimilarity measures. The similarity measure is based on the maximization of correlation between shapes, while the dissimilarity measure — on the minimization of the distance between shapes.

Let us take as an example two vectors  $V_A(a_1, a_2, \dots, A_N)$  and  $V_B(b_1, b_2, \dots, B_N)$ , which represent object  $A$  and object  $B$  in a  $N$ -dimensional feature space. The Euclidean distance  $d_E$  between these two vectors is defined by means of the following formula [11]:

$$d_E(V_A, V_B) = \sqrt{\sum_{i=1}^N (a_i - b_i)^2}. \quad (1)$$

The Mahalanobis distance  $d_M$  between vectors  $V_A$  and  $V_B$  can be derived as follows [7]:

$$d_M(V_A, V_B) = \sqrt{(V_A - V_B)^T E^{-1} (V_A - V_B)}, \quad (2)$$

where  $E^{-1}$  is the covariance matrix.

The correlation coefficient may be calculated both for the matrix and vector representations of a shape. The correlation between two matrices can be derived using the formula [16]:

$$c_c = \frac{\sum_m \sum_n (A_{nm} - \bar{A})(B_{nm} - \bar{B})}{\sqrt{\left(\sum_m \sum_n (A_{nm} - \bar{A})^2\right) \left(\sum_m \sum_n (B_{nm} - \bar{B})^2\right)}}, \quad (3)$$

where:

$A_{mn}, B_{mn}$  — pixel value with coordinates  $(m, n)$ , respectively in image  $A$  and  $B$ ,

$\bar{A}, \bar{B}$  — average value of all pixels, respectively in image  $A$  and  $B$ .

The C1 metric is also a similarity measure based on shape correlation. It is obtained by means of the following formula [12]:

$$c_1(A, B) = 1 - \frac{\sum_{i=1}^H \sum_{j=1}^W |a_{ij} - b_{ij}|}{\sum_{i=1}^H \sum_{j=1}^W (|a_{ij}| + |b_{ij}|)} \quad (4)$$

where:

$A, B$  — matched shape representations,  
 $H, W$  — height and width of the representation.

### 3 Selected Shape Descriptors

#### 3.1 Two-Dimensional Fourier Descriptor

The use of Fourier-based shape descriptors is widespread in pattern recognition and valued for its properties, including shape generalisation, robustness to noise, scale invariance and translation invariance. The Two-Dimensional Fourier Descriptor (2DFD) has the form of a matrix with absolute complex values, and is derived as follows [9]:

$$C(k, l) = \frac{1}{HW} \left| \sum_{h=1}^H \sum_{w=1}^W P(h, w) \cdot \exp(-i \frac{2\pi}{H} (k-1)(h-1)) \dots \dots \exp(-i \frac{2\pi}{W} (l-1)(w-1)) \right|, \quad (5)$$

where:

$H, W$  — height and width of the image in pixels,  
 $k$  — sampling rate in vertical direction ( $k \geq 1$  and  $k \leq H$ ),  
 $l$  — sampling rate in horizontal direction ( $l \geq 1$  and  $l \leq W$ ),  
 $C(k, l)$  — value of the coefficient of discrete Fourier transform in the coefficient matrix in  $k$  row and  $l$  column,  
 $P(h, w)$  — value in the image plane with coordinates  $h, w$ .

#### 3.2 UNL-Fourier

The UNL-Fourier (UNL-F) descriptor is composed of the UNL (named after Universidade Nova de Lisboa) descriptor and Fourier transform. The UNL utilizes a complex representation of Cartesian coordinates for points and parametric curves in discrete manner [17]:

$$z(t) = (x_1 + t(x_2 - x_1)) + j(y_1 + t(y_2 - y_1)), \quad t \in (0, 1), \quad (6)$$

where  $z_1 = x_1 + jy_1$  and  $z_2 = x_2 + jy_2$  are complex numbers. In the next step, the centroid  $O$  is calculated [17]:

$$O = (O_x, O_y) = \left( \frac{1}{n} \sum_{i=1}^n x_i, \frac{1}{n} \sum_{i=1}^n y_i \right), \quad (7)$$

and the maximal Euclidean distance between contour points and centroid is found [17]:

$$M = \max_i \{ \|z_i(t) - O\| \} \quad \forall i = 1 \dots n \quad t \in (0, 1). \quad (8)$$

Based on the above formulations, a discrete version of the new coordinates is calculated as follows [17]:

$$U(z(t)) = \frac{\| (x_1 + t(x_2 - x_1) - O_x) + j(y_1 + t(y_2 - y_1) - O_y) \|}{M} + j \times \arctan \left( \frac{y_1 + t(y_2 - y_1) - O_y}{x_1 + t(x_2 - x_1) - O_x} \right). \quad (9)$$

Original pixel values are put into a square Cartesian matrix based on the new coordinates. This results in an image containing unfolded shape contour in polar coordinates, in which rows represent distances from the centroid and columns — the angles. As a result, the 2DFD can be applied.

#### 3.3 Generic Fourier Descriptor

The Generic Fourier Descriptor (GFD) utilizes the transformation of a region shape to the polar coordinate system. It means that all pixel coordinates of an original image are transformed into polar coordinates. Next, the original pixel values are put to new coordinates on a rectangular Cartesian image, in which the row elements correspond to distances from the centroid and the columns to angles [13]. Again, the result is two-dimensional and the Fourier transform can be applied.

#### 3.4 Point Distance Histogram

The Point Distance Histogram (PDH) is a shape descriptor that utilizes information about the shape contour. In order to derive a PDH representation, an origin of the polar transform of a contour is firstly selected, usually a centroid  $O$ . Polar coordinates are stored in two vectors —  $\Theta^i$  for angles and  $P^i$  for radii [3]:

$$\Theta_i = a \tan \left( \frac{y_i - O_y}{x_i - O_x} \right), \quad (10)$$

$$P_i = \sqrt{(x_i - O_x)^2 + (y_i - O_y)^2}. \quad (11)$$

In the next step, the values in  $\Theta^i$  are converted to the nearest integers. Then the elements in  $\Theta^i$  and  $P^i$  are rearranged with respect to the increasing values in  $\Theta^i$ , and denoted as  $\Theta^j, P^j$ . If there are any equal elements in  $\Theta^j$ , then only the element with the highest value in  $P^j$  is left. Next, only the  $P^j$  vector is selected for further processing and denoted as  $P^k$ , where  $k = 1, 2, \dots, m$  and  $m \leq 360$ . The elements of  $P^k$  vector are normalized and assigned to bins in the histogram ( $\rho_k$  to  $l_k$ ) [3]:

$$l_k = \begin{cases} r, & \text{if } \rho_k = 1 \\ \lfloor r \rho_k \rfloor, & \text{if } \rho_k \neq 1 \end{cases} \quad (12)$$

where  $r$  is a previously determined number of bins. In the next step, the values in the histogram bins are normalized according to the highest one. Ultimately, the final histogram which represents a shape is obtained and can be written as the following function  $h(l_k)$  [3]:

$$h(l_k) = \sum_{k=1}^m b(k, l_k), \quad (13)$$

where [3]:

$$b(k, l_k) = \begin{cases} 1, & \text{if } k = l_k \\ 0, & \text{if } k \neq l_k \end{cases} \quad (14)$$

### 3.5 Zernike Moments

Zernike Moments (ZM) are orthogonal moments. Among the advantages of this descriptor are rotation invariance, robustness to noise and minor variations in shape. The complex Zernike Moments are derived from orthogonal Zernike polynomials, which are a set of functions orthogonal over the unit disk  $x^2 + y^2 < 1$ . The Zernike Moments of order  $n$  and repetition  $m$  of a region shape  $f(x, y)$  can be obtained by the following formula [13]:

$$Z_{nm} = \frac{n+1}{\pi} \sum_r \sum_{\theta} f(r \cos \theta, r \sin \theta) \cdot R_{nm}(r) \cdot \exp(jm\theta), \quad (15)$$

$$r \leq 1.$$

where  $R_{nm}(r)$  is the orthogonal radial polynomial [13]:

$$R_{nm}(r) = \sum_{s=0}^{(n-|m|)/2} (-1)^s \dots \dots \frac{(n-s)!}{s! \times \left(\frac{n-2s+|m|}{2}\right)! \left(\frac{n-2s-|m|}{2}\right)!} r^{n-2s}, \quad (16)$$

where  $n = 0, 1, 2, \dots; 0 \leq |m| \leq n; n - |m|$  is even.

## 4 The Description of the Experiments and Experimental Results

During the experiments, five different shape descriptors and four matching methods were used. In each experiment, one combination of a shape descriptor and matching method was investigated. Firstly, all shapes were represented using a selected variant of the shape descriptor — a feature vector, i.e. part of the absolute spectrum in case of 2DFD, GFD or UNL-F, various orders for ZM and various number of histogram bins for PDH. Next, the representations of test objects were matched with the representations of templates by calculating the similarity or dissimilarity measure. Lastly, one most similar template was selected for each investigated object, giving a set of templates.

At this point it is important to take a closer look at the data and shape representations. The shapes that were used

in the experiments are depicted in Fig. 1 and consisted of  $200 \times 200$  pixel size images with a white background and black silhouettes of similar size placed in the middle. The shapes consisted of ten shapes that were general templates (the first row in Fig. 1) and test objects. The shape representations varied significantly in terms of size. In case of shape descriptors based on the Fourier transform, various parts of the original absolute spectrum were investigated, namely  $2 \times 2$ ,  $5 \times 5$ ,  $10 \times 10$ ,  $25 \times 25$  and  $50 \times 50$  subparts of the coefficient matrix. Each block was transformed into a vector to form a final shape representation. The Zernike Moments descriptor was calculated for orders from 1 to 20, what resulted in feature vectors having from 2 to 121 elements. The Point Distance Histogram descriptor had seven variants that were obtained for 2, 5, 10, 25, 50, 75 and 100 histogram bins, and simultaneously produced feature vectors of size equal to the number of bins.

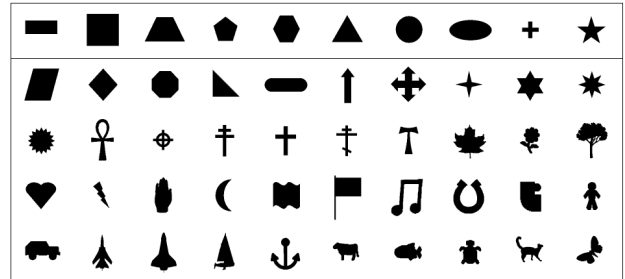


Figure 1: Shapes used in the experiments divided into 10 templates (first row) and 40 test objects (rest) [3].

The effectiveness of the experiment was estimated by calculating the percentage of the templates selected in the experiment that was consistent with the templates indicated by people in the inquiries concerning the same GSA task. In the inquiry people were asked to indicate five most similar templates for all test objects and arrange them from the most to the least similar one. In the paper, for an individual test object, only three out of five templates were taken into account and are compared with one template resulted from the experiments — here the sequence of indications is not taken into account. Templates indicated by people are provided in Fig. 2. The percentage differences of indications between the most and the second most similar templates are various and depend on the test object. For instance, for test object no. 14 a cross template was indicated by 65% of people and the star template by 64%. In case of test object no. 4 the difference was greater — 94% of people indicated a triangle and 46% indicated trapeze.

The aim of the experiments was to select the combination of a shape descriptor and matching method that gave the highest effectiveness and, additionally, in the case of several combinations with the same percentage effectiveness, in which the size of the shape representation would be the smallest. The following part of this section describes the experimental results.

The first set of the experiments utilized the Two-

No.	Test object	Templates			No.	Test object	Templates		
		1	2	3			1	2	3
1					21				
2					22				
3					23				
4					24				
5					25				
6					26				
7					27				
8					28				
9					29				
10					30				
11					31				
12					32				
13					33				
14					34				
15					35				
16					36				
17					37				
18					38				
19					39				
20					40				

Figure 2: Templates most frequently indicated by people in the inquiries.

Dimensional Fourier Descriptor and five different absolute spectrum subparts. The percentage effectiveness values for each combination of a shape descriptor and matching method are provided in Fig. 3. As can be seen in Fig. 3, the effectiveness values vary significantly and the weakest results were achieved in case of the use of the Mahalanobis distance. The highest effectiveness was obtained in the case of combinations with the percentage value equal to 55%. The best result can be attributed to the  $5 \times 5$  subpart of the 2DFD and both similarity measures — correlation coefficient and C1 metric.

In the second set of the experiments, the Generic Fourier Descriptor was used and again five absolute spectrum subparts were investigated (see Fig. 4). Compared to the previous experiment, the best result was obtained using a dissimilarity measure — the Euclidean distance, and the smallest feature vector —  $2 \times 2$  subpart of the absolute spectrum. Similarly as in the previous case, the Mahalanobis distance provided the lowest effectiveness values.

The third set of the experiments included the application of the UNL-Fourier descriptor and again various subparts

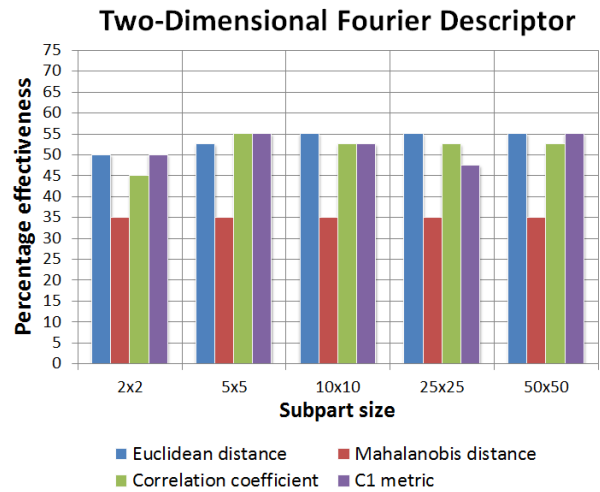


Figure 3: Bar chart representing the experiment results using the 2DFD.

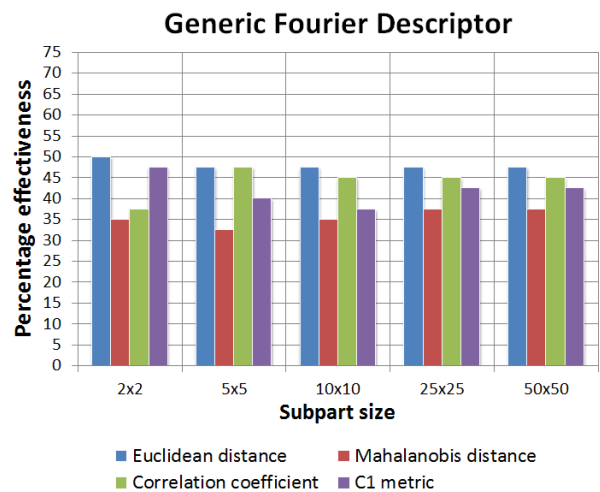


Figure 4: Bar chart representing the experiment results using the GFD.

of the Fourier coefficient matrix. The results are provided in Fig. 5. Three combinations stood out —  $2 \times 2$  and  $5 \times 5$  subparts of the UNL-F, which were matched using Euclidean distance, and  $2 \times 2$  subpart of the UNL-F matched using C1 metric. These combinations gave 62,5% twice and 70% respectively. It is worth noting that the smallest feature vectors were sufficient to distinguish templates from each other and indicate the templates consistent with human indications.

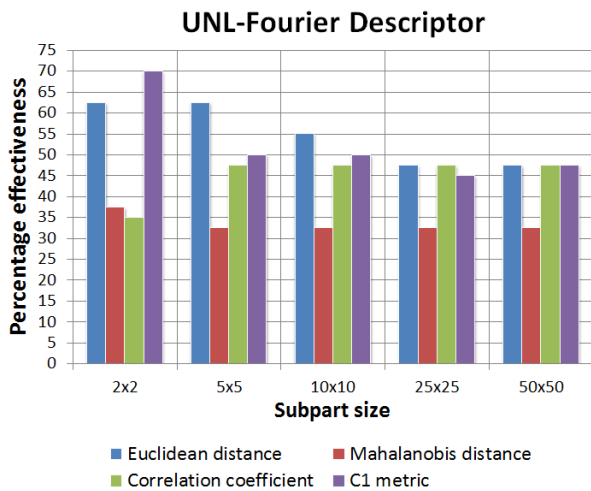


Figure 5: Bar chart representing the experiment results using the UNL-F.

The fourth set of experiments concerned the investigation of the effectiveness of Zernike Moments descriptor and different orders of moment were used (see Fig. 6). The results are varied — the percentage effectiveness values range from 22.5% to 60%. Surprisingly, the best results were observed when the Mahalanobis distance was applied as the matching method and the first-order moment was used. In this case the feature vector had only two elements.

The last set of the experiments examined the Point Distance Histogram descriptor. A different number of histogram bins was utilized, what resulted in a varying number of elements in each feature vector. As can be seen in Fig. 7, the highest effectiveness value was equal to 50% and was obtained for the combination of the PDH descriptor calculated for five histogram bins and C1 metric.

## 5 Conclusions

The paper covered the problem of the General Shape Analysis and investigated some solutions to it. Firstly, the idea underlying the approach was introduced and its possible applications, as well as several methods and algorithms that are already in use were briefly presented. In solving the GSA problem we are establishing the degree of similarity between test objects and general templates — one or few templates, which are most similar to an inves-

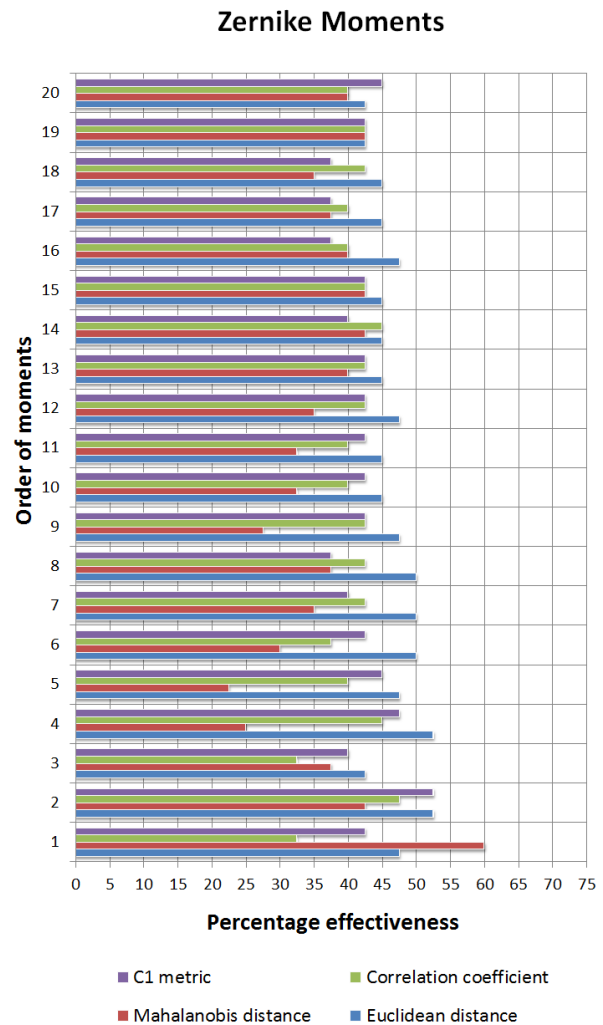


Figure 6: Bar chart representing the experiment results using the ZM.

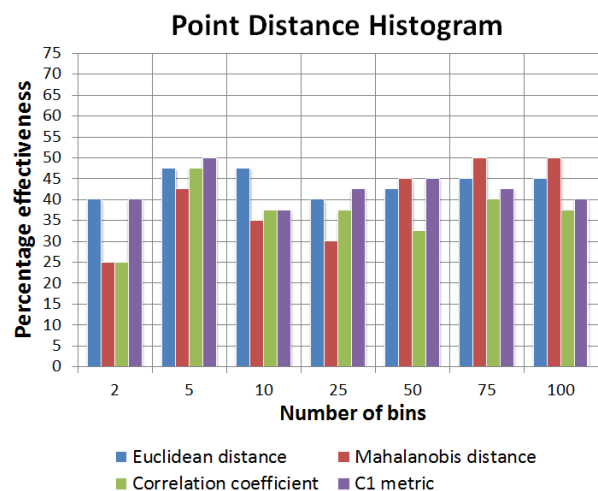


Figure 7: Bar chart representing the experiment results using the PDH.

tigated object are selected and compared with benchmark results in order to estimate the effectiveness of the experiment. The main goal of the experiments presented in the paper was to examine various combinations of shape descriptors and matching methods. Five shape descriptors were used to calculate shape representations (feature vectors) of various size. The descriptors comprised the Two-Dimensional Fourier Descriptor, Generic Fourier Descriptor, UNL-Fourier, Zernike Moments and Point Distance Histogram. The matching methods included two similarity measures, namely the correlation coefficient and C1 metric, and two dissimilarity measures — the Euclidean and Mahalanobis distances. Based on the experimental results, the best solution for the GSA problem was selected, i.e. a combination of a shape descriptor and matching method, which gave the highest percentage effectiveness. What is more, the smaller the feature vector the better the result. On the basis of the abovementioned criteria, the best solution for the GSA problem is the combination of the UNL-F descriptor,  $2 \times 2$  subpart of the absolute spectrum and C1 metric. Pictorial results are provided in Fig. 8. Additionally, both the calculation of description vectors (shapes and templates together) and similarity measures between shapes are not time-consuming. There are slight differences between runtimes when using various matching methods and previously calculated descriptors (see Fig. 9), however they are not significant for small-sized description vectors.

No.	Test object	Template	Test object	Template	No.	Test object	Template
1					29		
2					30		
3					31		
4					32		
5					33		
6					34		
7					35		
8					36		
9					37		
10					38		
11					39		
12					40		
13							
14							

Figure 8: Results of the best experiment using UNL-Fourier descriptor and C1 metric.

By way of conclusion, it needs to be highlighted that the matching method has a significant impact on the final effectiveness of the experiment. Moreover, the effectiveness values also depend on the applied version of the shape descriptor. In other words, taking into consideration solely

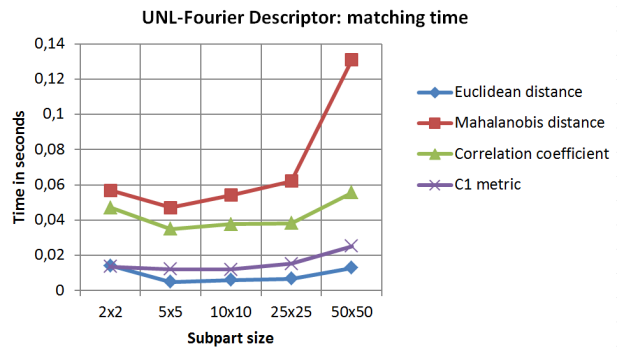


Figure 9: A comparison of matching times for various size of UNL-F Descriptor and matching methods.

one particular shape description algorithm, each combination of a feature vector and matching method produces different experimental results. This in turn may indicate that some feature vectors represent significant shape features in a more appropriate way, enabling easy recognition and matching of all shapes with common general characteristics. However, a matching method does not change the original efficiency of the shape description algorithm. A high diversity in effectiveness values stems from the fact that each matching method is based on different inputs, therefore it should be properly selected to fit the actual problem and the shape descriptor applied. Summarizing, three factors can affect the final experimental result: a shape description algorithm, the size of a feature vector and a method for estimating similarity between shape representations.

## References

- [1] Frejlichowski D. General shape analysis using fourier shape descriptors. In Swiatek J., Borzemski L., Grzech A., and Wilimowska Z., editors, *Information Systems Architecture and Technology — System Analysis in Decision Aided Problems*, pages 143–154. Oficyna Wydawnicza Politechniki Wrocławskiej, 2009.
- [2] Frejlichowski D. An experimental comparison of seven shape descriptors in the general shape analysis problem. In Campilho A. C. and Kamel M. S., editors, *ICIAR (1)*, volume 6111 of *Lecture Notes in Computer Science*, pages 294–305. Springer, 2010.
- [3] Frejlichowski D. An experimental comparison of three polar shape descriptors in the general shape analysis problem. In Swiatek J., Borzemski L., Grzech A., and Wilimowska Z., editors, *Information Systems Architecture and Technology — System Analysis in Decision Aided Problems*, pages 139–150. Oficyna Wydawnicza Politechniki Wrocławskiej, 2010.

- [4] Frejlichowski D. Application of zernike moments to the problem of general shape analysis. *Control and Cybernetics*, vol. 40, no. 2:515–526, 2011.
- [5] Frejlichowski D. Application of the curvature scale space descriptor to the problem of general shape analysis. *Przegląd Elektrotechniczny (Electrical Review)*, no. 10b/2012:209–212, 2012.
- [6] Frejlichowski D. and Gościewska K. Application of 2d fourier descriptors and similarity measures to the general shape analysis problem. In Bolc L., Tadeusiewicz R., Chmielewski L. J., and Wojciechowski K. W., editors, *ICCVG*, volume 7594 of *Lecture Notes in Computer Science*, pages 371–378. Springer, 2012.
- [7] Zhang D. *Image Retrieval Based on Shape*. Dissertation, Faculty of Information Technology, Monash University, Australia, 2002.
- [8] Luciano da Fontoura Costa and Roberto Marcond Cesar Jr. *Shape Analysis and Classification: Theory and Practice*. CRC Press, 2000.
- [9] Kukharev G. *Digital Image Processing and Analysis (in Polish)*. SUT Press, 1998.
- [10] Biederman I. Recognition-by-components: A theory of human image understanding. *Psychological Review*, vol. 94, no. 2:115–147, 1987.
- [11] Kpalma K. and Ronsin J. An overview of advances of pattern recognition systems in computer vision. In Obinata G. and Dutta A., editors, *Vision Systems: Segmentation and Pattern Recognition*. I-Tech, Vienna, Austria, 2007.
- [12] Lam K.-M. and Yan H. An analytic-to-holistic approach for face recognition based on a single frontal view. *Pattern Analysis and Machine Intelligence, IEEE Transactions on*, 20(7):673–686, Jul 1998.
- [13] Yang M., Kpalma K., and Ronsin J. A survey of shape feature extraction techniques. In Peng-Yeng Yin, editor, *Pattern Recognition*, pages 43–90. I-Tech, Vienna, Austria, 2008.
- [14] Forcmański P. and Frejlichowski D. Robust stamps detection and classification by means of general shape analysis. In Bolc L., Tadeusiewicz R., Chmielewski L. J., and Wojciechowski K. W., editors, *ICCVG (1)*, volume 6374 of *Lecture Notes in Computer Science*, pages 360–367. Springer, 2010.
- [15] Youguo Pi, Wenzhi Liao, Mingyou Liu, and Jianping Lu. Theory of cognitive pattern recognition. In Peng-Yeng Yin, editor, *Pattern Recognition Techniques, Technology and Applications*. I-Tech, Vienna, Austria, 2008.
- [16] Chwastek T. and Mikrut S. The problem of automatic measurement of fiducial mark on air images (in polish). *Archives of Photogrammetry, Cartography and Remote Sensing*, 16:125–133, 2006.
- [17] Rauber T. W. Two dimensional shape description. Technical report, Universidade Nova de Lisboa, Lisboa, Portugal, 1994.